Journal of Hazardous Materials 194 (2011) 209–215

Contents lists available at ScienceDirect

Journal of Hazardous Materials

journal homepage: www.elsevier.com/locate/jhazmat

Size-dependent enrichment of waste slag aggregate fragments abraded from asphalt concrete

Fumitake Takahashi[a,*], Takayuki Shimaoka[a], Kevin Gardner[b], Akiko Kida[c]

[a] Faculty of Urban and Environmental Engineering, Graduate School of Engineering, Kyushu University, 744 Motooka, Nishi-ku, Fukuoka 819-0395, Japan
[b] Environmental Research Group, University of New Hampshire, 336 Gregg Hall, 35 Colovos Road, Durham, New Hampshire 03824-3534, USA
[c] Research Center for Material Cycles and Waste Management, National Institute for Environmental Studies, 16-2 Onogawa, Tsukuba 305-8505, Japan

ARTICLE INFO

Article history:
Received 6 August 2010
Received in revised form 2 July 2011
Accepted 25 July 2011
Available online 5 August 2011

Keywords:
Waste slag
Asphalt pavement
Aggregate
Abrasion dust
Enrichment

ABSTRACT

Authors consider the environmental prospects of using melted waste slag as the aggregate for asphalt pavement. In particular, the enrichment of slag-derived fragments in fine abrasion dust particles originated from slag asphalt concrete and its size dependency were concerned. A series of surface abrasion tests for asphalt concrete specimens, containing only natural aggregates as reference or 30 wt% of substituted slag aggregates, were performed. Although two of three slag-asphalt concretes generated 1.5–3.0 times larger amount of abrasion dust than the reference asphalt concrete did, it could not be explained only by abrasion resistance of slag. The enrichment of slag-derived fragments in abrasion dust, estimated on the basis of the peak intensity of quartz and heavy metal concentrations, had size dependency for all slag-asphalt concretes. Slag-derived fragments were enriched in abrasion dust particles with diameters of 150–1000 μm. Enrichment factors were 1.4–2.1. In contrast, there was no enrichment in abrasion dust particles with diameter less than 75 μm. This suggests that prior airborne-size fragmentation of substituted slag aggregates does not need to be considered for tested slag aggregates when environmental risks of abrasion dust of slag-asphalt pavement are assessed.

© 2011 Elsevier B.V. All rights reserved.

1. Introduction

In Japan, waste management, especially disposal capacity management of landfill sites, is one of severe social problems owing to large difficulty to build new landfill sites. Waste slags including steel-making slag and vitrificated residues of municipal solid waste (MSW slag) are one of major wastes which are landfilled. In 2006, 685 thousand tons of steel-making slag and 294–368 thousand tons of MSW slag were disposed to landfill sites in Japan. Recently, melting treatment has been applied to other industrial wastes like automobile shredder residues (ASR), contaminated soil, and asbestos-containing demolition wastes for complete decomposition of toxic organic/inorganic compounds although melting treatment needs large energy consumption and high operational costs. Therefore, the utilization of waste slag like MSW slag, melted ASR slag, and melted contaminated soil slag will be requested strongly from the viewpoint of waste management in Japan. In this context, applications of waste slags to road asphalt aggregates have been greatly attractive. Waste slag applications as road asphalt aggregates have been investigated focusing on mechanical stability and durability of asphalt pavement for basic oxygen furnace slag [1,2], steel slag [3,4], and MSW slag [5]. In addition to mechanical stability and durability, emission of abrasion dust including airborne particulate matter (PM10 and PM2.5) has been also concerned from environmental viewpoint. The generation of abrasion dust from asphalt pavement is a complex mechanism. It depends on many factors such as the type of tire [6], characteristics of aggregates like size distribution [7,8], mechanical resistance [7], and surface microtexture [2,9] which are related with interlocking between slag aggregate and asphalt binder. This study focuses on the fragmentation of slag aggregates during asphalt pavement abrasion. If slag aggregates degrade to smaller particles than natural aggregates do, this means slag-derived fragments will be concentrated more highly in smaller abrasion dust particles. Because smaller dust particles increase the risk of inhalation intake and waste slag usually contains high concentrations of toxic heavy metals [10–16], the abrasion dust of slag-asphalt pavement might pose a non-negligible health risk as well as an environmental risk. As a necessary first step in assessing such risk, it should be investigated whether slag-derived fragments can be enriched highly in smaller dust during the abrasion of slag-asphalt concrete or not. Therefore, the objective of this study is to investigate the enrichment of slag-derived fragments in abrasion dust and its dependency on dust size. Such knowledge would help determine health and environmental risks of fine abrasion dust when slag aggregate is applied to asphalt pavement instead of natural aggregates.

* Corresponding author. Tel.: +81 92 802 3431; fax: +81 92 802 3432.
E-mail address: f-takahashi@doc.kyushu-u.ac.jp (F. Takahashi).

0304-3894/$ – see front matter © 2011 Elsevier B.V. All rights reserved.
doi:10.1016/j.jhazmat.2011.07.086

Table 1
Descriptions of slag and natural aggregates.

	Slag A	Slag B	Slag C	Natural aggregates (Crashed stone) (6/7 grade)
Waste source	Municipal solid wastes (MSW)	Automobile shredder residues (ASR)	Contaminated soil and industrial wastes	–
Pretreatment (incineration/gasification)	Kiln type gasification	Shaft-furnace type gasification	Rotary kiln type incineration	–
Melting facility type	Rotational flow type melting	Shaft-furnace type melting	Rotary surface melting	–
Melting temperature	1300	1700–1800	1250	–
Gas condition in melting zone	Reductive	Reductive	Reductive	–
Cooling and granulation method	Water cooling/granulation	Water cooling/granulation	Water cooling/granulation	–
Average diameter (mm)	6.4	6.2	6.5	6.3
Los Angles abrasion value (%)	49	51	68	19.6

2. Experimental

2.1. The relative share of slag-derived fragments in abrasion dust

The relative share of slag-derived fragments in size-distributed abrasion dust was investigated using two methods. One method is based on the mineralogical differences between melted waste slag and natural aggregates. Although crystalline SiO_2 (quartz) is a major component mineral in natural aggregates, the glassy and amorphous slag contains a negligible amount. Therefore, the peak intensity of quartz in X-ray diffraction analysis can be used to estimate the relative shares of slag-derived fragments in abrasion dust according to

$$X_{i,j} = 100 \cdot \left(1 - \frac{C_{i,j}}{A_j}\right) \quad (1)$$

where $X_{i,j}$ is the relative share of slag-derived fragments in abrasion dust (size range j) of slag (i) asphalt concrete. $C_{i,j}$ and A_j are quartz peak intensities of abrasion dust (size range j) of slag (i) asphalt concrete and of reference-asphalt concrete, respectively.

The other method is based on the differences in metal contents. In general, waste slag contains higher concentrations of heavy metals. These differences enable the estimation of the relative share according to

$$X_{i,j} = 100 \cdot \left(\frac{A_{i,j} - C_j}{B_i - C}\right) \quad (2)$$

where $A_{i,j}$ and C_j are the metal concentrations of abrasion dust (size range j) of slag (i) asphalt concrete and of reference-asphalt concrete, respectively. B_i and C are the metal concentrations of slag (i) and natural aggregates, respectively. Heavy metals, which have largely different concentrations between slag and natural aggregates, were focused on because a smaller difference in the heavy metal concentrations results in larger estimation errors. Results obtained using the two methods were compared to evaluate the reliability of the estimation.

2.2. The description of waste slag

Three types of waste slag were tested as aggregates. One is melted MSWI residue at 1300 °C using rotational flow type melting facility (slag A). Second slag is vitrified combustion ash of automotive shredder residue at 1750–1800 °C using shaft-furnace type melting facility (slag B). The last one is melted incineration residue of a contaminated soil and industrial waste mixture at 1250 °C using rotary surface melting type facility (slag C). All slags were generated under reductive conditions and then water-granulated. Detailed descriptions of these slag including average diameter and Los Angeles abrasion value are summarized in Table 1. Los Angeles abrasion values were measured by Japan Industry Standard method A1121 (JIS A1121). Average size and Los Angeles abrasion value of natural aggregates are also listed in Table 1. Natural aggregates used in this study were 6-grade and 7-grade crashed stone, which were defined by JIS A 5001-1988 and consisted mainly of andesite and sandstone. Aggregate size ranges were 2.5–5.0 mm for 6-grade stone and 5.0–13 mm for 7-grade stone, respectively. It must be noted that the uncertainty of Los Angeles abrasion values for all slag samples might be non-negligible. Although JIS A1121 abrasion test requests 5 ± 0.01 kg of samples, only 1–2 kg of the same lot slag samples could be tested.

2.3. Quartz in waste slag and natural aggregates

Quartz peak intensities ($2\Theta = 26.7°$) of waste slags, natural aggregates, and abrasion dust were measured using an X-ray diffraction analyzer (XRD: RIGAKU Co., UltimaIII). Because quartz peak intensity of natural aggregates depends strongly on their mineralogical properties, it was confirmed before the preparation of asphalt concretes and was enough for relative share estimation. To estimate the relative share of slag-derived fragments in abrasion dust on the basis of quartz peak intensity, a standard curve was prepared. 0–50 wt% of powdered SiO_2 reagent (Wako Co., purity >99%) was mixed with slag powder for standard curve samples.

2.4. Metal content

All samples were ground to less than 150 μm and dried before analysis. 0.1–0.3 g of sample were mixed with 3 g of lithium metaborate in a platinum dish. This mixture was heated at 850 °C in an oven for 3 h. The melted mixture was cooled and digested by 100 ml of 3 M nitric acid. After digestion, sample solutions were analyzed by inductively coupled plasma atomic emission spectroscopy (ICP-AES: SII-NT Co., SPS5510) and inductively coupled plasma mass spectroscopy (ICP-MS: SII-NT Co., SPQ9700).

2.5. Slag-asphalt and reference concretes

The compositions of slag-asphalt concretes and reference asphalt concretes are given in Table 2. It should be noted that "AC" described in tables or figures means asphalt concrete. Asphalt concrete using only natural aggregates was used as a reference. One of the three waste slags (slags A, B, and C) or coarse sand was used as the aggregate in each case. The content of coarse sand or substituted slag was 30 wt% and their size distributions were almost the same as shown in Fig. 1. Size distributions of natural and slag aggregates were adjusted for comparison and are shown in Fig. 2.

Table 2
Compositions of reference and slag asphalt concretes (unit: %).

	Reference AC	Slag A AC	Slag B AC	Slag C AC
Crashed stone (6 grade)	33	33	33	33
Crashed stone (7 grade)	22	25	18	25
Screanings	10	7	13	7
Coarse sand	30	–	–	–
Stone powder	5	5	6	5
Slag	–	30	30	30
Asphalt binder	5	5	5	5

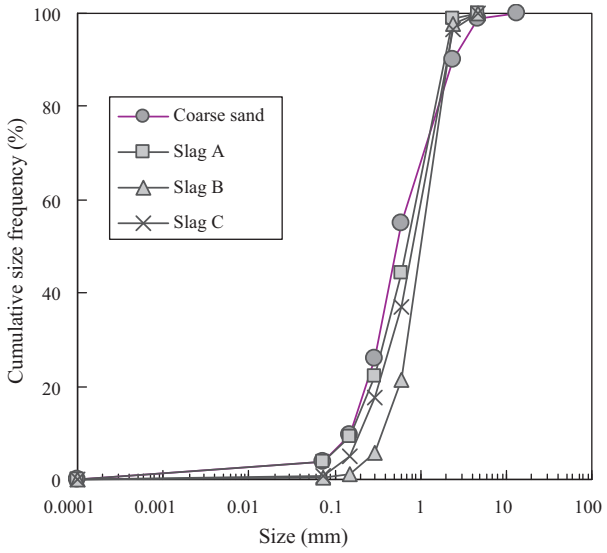

Fig. 1. Size distribution of coarse sand and melted waste slag (slags A, B, and C).

After 15 cm × 40 cm × 5 cm specimens of the reference and slag-asphalt concretes were made, they were stabilized for 5 h under room condition. After that, they were used for surface abrasion tests.

2.6. Surface abrasion test

Surface abrasion was conducted using the "raveling test" method based on a Japanese standard pavement test (Hosoubinran 3-7-2). A wheel tire covered with a stainless steel chain revolved on asphalt concrete plates at 200 rpm for 3 h and abraded the surface. The air temperature was kept at −10 °C during the abrasion. The experimental apparatus of the raveling test is shown in Fig. 3. After all abrasion dust was recovered, the asphalt binder contained in the abrasion dust was removed by the Soxhlet extraction method (medium: trichloroethylene). The size distribution of the abrasion dust was then measured by sieving and precipitation tests based on JIS Z 8901 method. After all dust was sieved to less than 75 μm, 75–150 μm, 150–300 μm, 300–600 μm, 600 μm to 1.0 mm and more than 1.0 mm, they were used for the quartz peaks analysis and metal contents measurement.

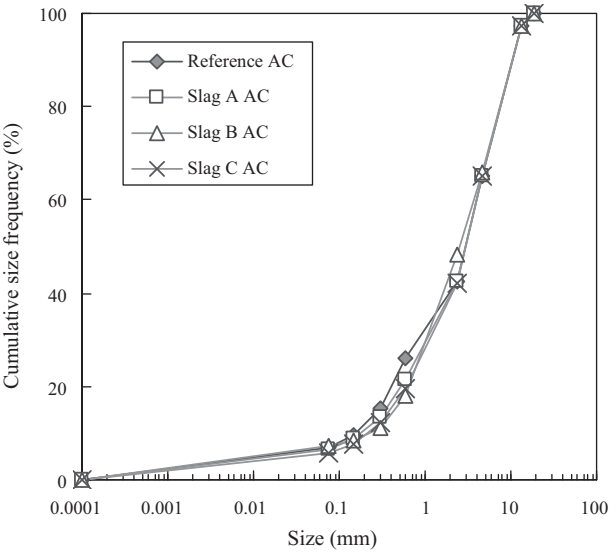

Fig. 2. Size distribution of aggregates of reference and slag asphalt concretes.

Fig. 3. The apparatus of surface abrasion test ("raveling test" method based on Japanese standard pavement tests (Hosoubinran 3-7-2)).

3. Results and discussion

3.1. Dust generation rate and size distribution

The amounts of abrasion dust for reference and slag-asphalt concretes are compared in Fig. 4. Dust sizes were categorized as less than 1.6 μm, 1.6–10.8 μm, 10.8–75 μm and more than 75 μm. If abrasion resistance of aggregates have dominant impacts on the

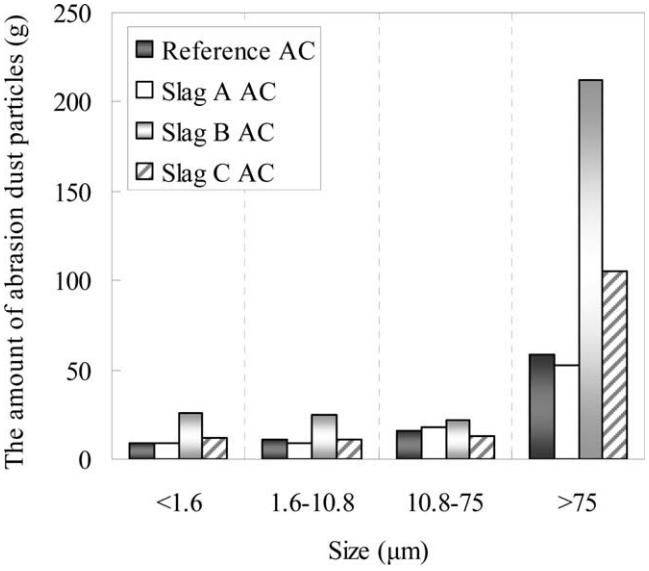

Fig. 4. Amount of abrasion dust particles for reference and slag-asphalt concretes.

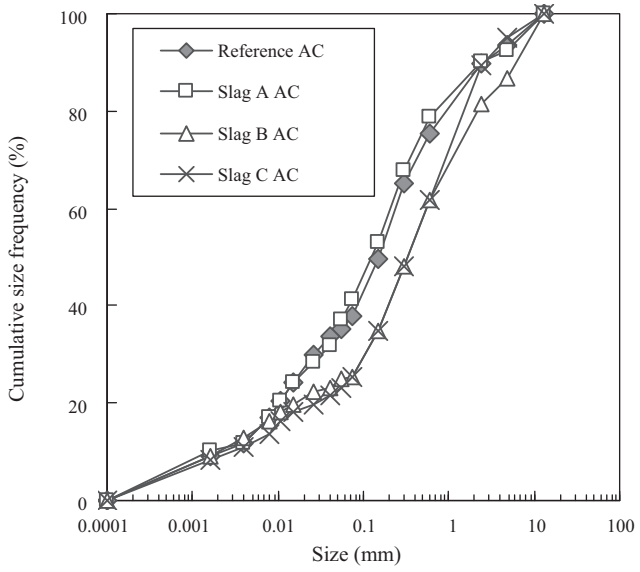

Fig. 5. Size distribution of abrasion dust particles for reference and slag-asphalt concretes.

generation rate of abrasion dust, slag-asphalt concretes, in particular slag C asphalt concrete, generate larger amount of abrasion dust than that of reference asphalt concrete because all types of slag had poor abrasion resistance than natural aggregate (see Table 1). However, experimental results are quite different from this expectation. Generation rates of abrasion dust for slag A asphalt concrete were almost the same as those for the reference asphalt concrete in each size category. Slag B and slag C asphalt concretes generated 3.0 and 1.5 times larger total amount of abrasion dust than that of reference asphalt concrete, respectively. These results cannot be explained only by abrasion resistance of aggregates and indicate other significant factors. Size distributions of abrasion dust for the reference and slag-asphalt concretes also suggest the necessity to consider not only abrasion resistance but also other significant factors on slag aggregate fragmentation. Size distributions of abrasion dust are shown in Fig. 5. Although poor abrasion resistance seemed to promote the generation of abrasion dust with smaller diameter, slag B and slag C asphalt concretes generated larger size of dust particles than the reference concrete did. In addition, there is no significant difference in size distribution of abrasion dust between slag A asphalt concrete and reference asphalt concrete. As mentioned in Section 1, interlocking between slag aggregate and asphalt binder, which is related to surface microtexture [2,9], is one of possible significant factors to explain these experimental results. Poor interaction between slag B/C and the asphalt binder might explain both higher generation rate of abrasion dust particles and larger size distribution. If slag B/C aggregates and/or its degraded fragments are released more easily from asphalt concrete compared with natural aggregates owing to their poor anchoring ability, this will yield a higher rate of dust emission. In addition, this gives slag aggregates less opportunity to be ground into smaller fragments by abrasion. Further study focusing on interlocking structure formed in asphalt concrete matrices is necessary for the verification.

3.2. Relative share of slag-derived fragments based on the quartz peak

Quartz peak intensities of abrasion dust generated from slag-asphalt and reference-asphalt concretes are illustrated in Fig. 6. Quartz peak intensity of reference abrasion dust had particle-size dependency and ranged from 12 000 to 17 000 cps. The highest peak

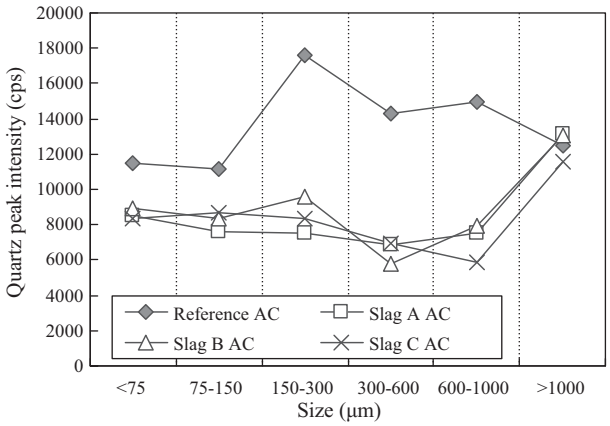

Fig. 6. Peak intensity of quartz in abrasion dust of reference and slag asphalt concretes.

Table 3
The relative share of slag-derived fragments in abrasion dust estimated on the basis of quartz peak intensity (unit: %).

Size (μm)	Slag A AC	Slag B AC	Slag C AC
<75	25.8	22.5	27.3
75–150	32.2	25.3	22.3
150–300	57.4	45.7	52.5
300–600	52.2	59.4	51.5
600–1000	49.6	47.2	60.9
>1000	0[a]	0[a]	7.2

[a] It is assumed to be zero because calculation results were negative values.

appeared in dust size of 150–300 μm. The average peak intensity, which was weighted based on size distribution shown in Fig. 6, was 13 023 cps for reference dust. Because slag-asphalt concretes contain 30 wt% substituted slag aggregates and the quartz peak intensity of slag aggregates is negligible, the weighted average of the quartz peak intensity for abrasion dust of slag-asphalt concretes should be 9116 cps, which is 70% of weighted-average peak intensity for reference dust. The weighted averages were 8906 cps for slag A asphalt concrete, 9863 cps for slag B asphalt concrete, and 9069 cps for slag C asphalt concrete. They were within 8.2% errors of the expected intensity (9116 cps) in all cases. This indicates good reliability of the estimation based on the quartz peak intensity. Estimation results are summarized in Table 3 and shown in Fig. 7. In the cases of slag A and B asphalt concrete dust particles with diameter of more than 1 mm, relative shares of slag-derived fragments were assumed to be 0% because calculated shares were less

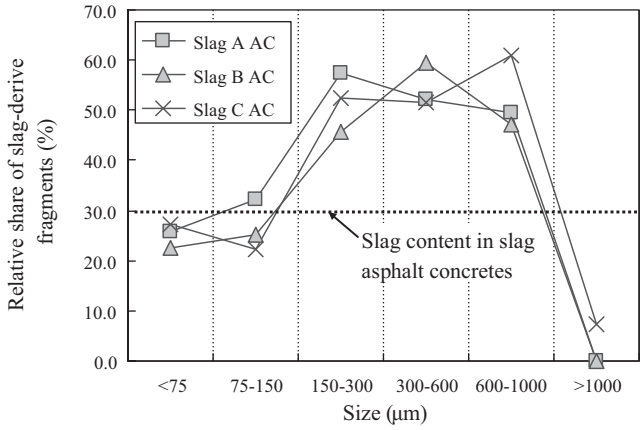

Fig. 7. Relative share of slag-derived fragments estimated on the basis of quartz peak intensity.

Table 4
Metal concentrations of aggregates and abrasion dust (unit: mg/kg), and recovery ratios of metals.

	Size (μm)	SD[a]	Al	Ba	Ca	Cr	Cu	Fe	K	Mg	Mn	Na	Ni	Pb	Sr	Ti	Zn
Natural aggregate	–	–	60 100	596	25 300	50.2	114	30 700	38 400	7600	427	25 900	100	16.1	157	2690	213
Slag A	–	–	86 300	630	175 000	1440	2130	26 500	33 500	19 300	967	37 600	96.9	220	337	7430	2110
Slag B	–	–	106 000	7170	206 000	283	3210	10 700	1250	21 200	529	18 500	99.2	31.1	1150	6300	94.3
Slag C	–	–	60 400	1180	127 000	1120	8380	69 200	26 800	7920	912	26 800	285	263	280	4240	1400
Reference AC	<75	37.8	58 500	589	39 500	72.4	110	36 600	37 600	7380	467	24 800	187	18.8	177	2920	117
	75–150	11.7	58 100	576	17 300	49.5	148	41 800	36 800	7160	484	26 200	130	21.8	147	2750	160
	150–300	15.7	58 700	569	16 100	33.9	134	29 200	36 700	8500	455	26 200	45.7	18.7	143	2470	185
	300–600	10.1	59 000	599	16 000	29.8	61.8	21 400	37 200	7490	391	25 600	19.7	13.2	137	2350	196
	600–1000	3.3	60 100	632	15 800	33.2	38.6	19 100	39 200	6420	322	26 400	23.9	10.9	138	2440	391
	>1000	21.4	65 800	634	17 200	35.4	126	21 400	42 100	7790	338	27 400	21.1	8.23	151	2620	412
Slag A AC	<75	41.2	61 800	575	69 600	354	439	39 300	37 600	10 000	539	27 600	169	41.5	206	4740	425
	75–150	11.8	66 400	565	78 400	575	749	46 900	36 900	11 500	659	32 000	174	75.7	213	4250	778
	150–300	14.9	70 500	585	90 000	693	1090	27 100	36 900	13 100	599	34 100	113	89.9	232	4750	931
	300–600	10.8	71 500	599	98 500	767	1190	21 900	37 100	14 100	591	34 400	72.4	91.0	241	5140	986
	600–1000	0.6	70 600	611	90 700	769	1010	21 100	37 300	13 500	555	34 000	65.5	82.9	231	4690	835
	>1000	20.7	63 000	590	47 600	314	472	18 000	38 100	9640	405	29 400	36.7	44.9	198	3070	370
Slag B AC	<75	25.5	67 200	1850	86 200	121	298	22 800	32 500	11 100	376	25 100	113	19.0	392	3570	58.8
	75–150	9.2	71 800	2750	91 400	119	739	17 200	26 500	12 700	352	25 100	51.5	12.2	513	3770	65.3
	150–300	13.5	75 300	3180	10 3000	139	1620	13 300	23 300	14 000	363	24 700	50.0	10.2	565	4020	78.6
	300–600	13.6	81 300	3770	124 000	154	1720	12 100	20 300	16 000	396	24 700	35.2	8.62	656	4620	68.8
	600–1000	0.80	79 100	3540	115 000	192	1460	12 000	21 700	15 400	383	24 400	27.8	5.32	621	4470	58.9
	>1000	37.4	67 300	1570	51 000	71.6	598	14 800	34 700	10 200	308	25 900	21.7	7.62	317	2870	47.9
Slag C AC	<75	25.5	56 700	814	67 800	319	686	40 100	35 100	8230	496	25 200	253	41.1	221	4020	320
	75–150	9.2	56 700	946	73 400	481	2900	41 800	32 700	7810	524	26 800	455	88.9	227	3490	666
	150–300	13.5	58 700	1090	81 700	590	4440	45 200	32 000	8120	592	27 900	327	113	241	3890	893
	300–600	13.6	60 500	1180	85 000	634	8130	46 100	31 700	8520	606	28 300	538	161	247	4400	890
	600–1000	4.4	61 100	1170	79 800	543	2530	39 500	33 400	8700	546	28 400	83.9	89.8	240	4380	821
	>1000	33.8	61 100	829	43 700	244	513	26 500	38 300	8320	388	27 300	40.0	33.9	189	2930	403
Recovery ratio (–)	Slag A AC	–	0.96	0.96	1.03	1.01	0.92	1.09	1.02	1.00	0.92	1.03	1.24	0.77	1.01	1.06	0.76
	Slag B AC	–	0.96	0.89	1.02	0.91	0.80	0.67	1.09	1.03	0.76	1.07	0.53	0.55	0.96	0.94	0.33
	Slag C AC	–	0.98	1.21	1.16	1.07	0.94	0.88	1.00	1.07	0.86	1.03	1.55	0.79	1.12	1.16	0.98

[a] Size distribution (unit: %).

Table 5
Selected elements for the calculation of relative share.

	Selected element for calculation
Slag A AC	Ca, Cr, Cu, Mg, Mn, Pb, Sr, Ti, Zn
Slag B AC	Al, Ba, Ca, Cr, Cu, K, Mg, Sr, Ti
Slag C AC	Ca, Cr, Cu, Fe, Mg, Mn, Pb, Zn

than zero. When the dust particle diameter was less than 75 μm, relative shares of slag-derived fragments were less than 30% for all slag-asphalt concretes. This means no enrichment of slag-derived fragments. On the other hand, they exceeded 30% for all dust particles with diameters of 150 μm to 1 mm. Slag-derived fragments were enriched 1.5–2.0 times higher in abrasion dust compared to original slag asphalt concrete. Relative share estimations indicate that the natural aggregate was ground to dust particles with diameter of less than 75 μm prior to slag aggregates. This also suggests that preferential abrasion of slag aggregates into fine dust is an unlikely scenario, at least, for three types of slag tested.

3.3. Relative share of slag-derived fragments based on heavy metal concentration

Heavy metal concentrations of natural aggregates, slag aggregates, and abrasion dusts are summarized in Table 4. Size distributions of the abrasion dusts are also listed in Table 4. Average concentrations of heavy metals, which are weighted by size distribution, in abrasion dust should be equal to the heavy metal concentrations in slag-asphalt concrete from the viewpoint of substance balances. To evaluate experimental error, recovery ratios, which are ratios of the weighted average concentration of heavy metals in abrasion dust to the heavy metal concentration in slag-asphalt concrete, were calculated and are summarized in Table 4. Except for Fe, Mn, Ni, Pb, and Zn, the recovery ratios were close to 1. This shows the good reliability of abrasion experiments. Heavy metals, which have good recovery ratios within 25% error and large differences in their contents between slag and natural aggregates, were selected for estimating the relative share of slag-derived fragments in abrasion dust. Selected heavy metals are listed in Table 5. Ca, Cr and Cu were used in all cases. Estimation results are summarized in Table 6 and illustrated in Fig. 8. There were large differences among estimation results. For example, relative shares in slag C abrasion dust with a diameter of less than 75 μm were estimated to be 27.9% based on Ca and 7.0% based on Cu. In this estimation method, it is assumed that the heavy metal concentration of slag-derived fragments is constant and does not depend on the diameter of fragments. However, heavy metals exist heterogeneously inside amorphous structures as oxide, aluminosilicate and other minerals [11]. This heterogeneity might result in large uncertainty of estimation results. When the dust particle diameter was less than 75 μm or more than 1.0 mm, the averages of relative shares were less than 30% for all slag-asphalt concretes. On the other hand, they were more than or almost equal to 30% for all dust particles with diameters of 75 μm to 1 mm. Enrichment factors of slag-derived fragments in abrasion dust with diameter of 150 μm to 1 mm were calculated to be 1.4–2.1. This size dependency of the enrichment was also confirmed in the estimation results based on quartz peak intensity. The estimation based on heavy metal concentrations also suggests that preferential abrasion of slag aggregates into fine dust rather than natural aggregates is an unlikely scenario for all tested slag.

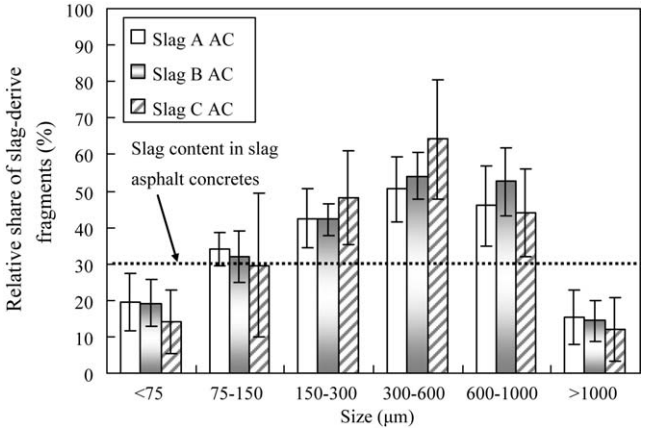

Fig. 8. Relative share of slag-derived fragments estimated on the basis of heavy metal concentration.

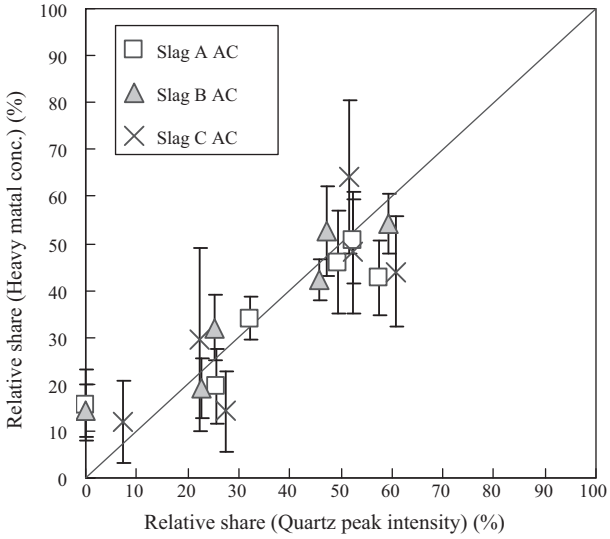

Fig. 9. Comparison of estimated relative shares of slag-derived fragments (quartz peak intensity vs heavy metal concentration).

3.4. Comparison of relative shares estimated using the two methods

Relative shares of slag-derived fragments in abrasion dust estimated on the basis of the quartz peak intensity and heavy metal concentration were compared. This comparison is illustrated in Fig. 9. The figure shows good agreement between the two estimations. In the case of slag C asphalt concrete, however, there were relatively large estimation errors. These errors were caused by a large difference between estimation results based on Fe, Mn, and Pb concentrations and those based on the quartz peak intensity. The poor substance balances for these elements implies larger uncertainty in the estimation based on their concentrations. Fine abrasion dust with diameter of less than 75 μm, which are most likely to be inhaled into human lung, were estimated by both methods to contain less than 30% of slag-derived fragments. This indicates that it is more difficult to degrade slag aggregates into fine dust than to degrade natural aggregates. Therefore, it is concluded that significant enrichment of slag-derived fragments in fine dust abraded from slag-asphalt concrete is not necessary to be considered for all tested slag when the environmental and health risks of such dust are assessed. Further study using other waste slag and focusing on interlocking structure formed in asphalt concrete matrices is a next step to verify no significant enrichment in airborne-size abrasion dust for other waste slag.

Table 6
Relative share of slag-derived fragments estimated on the basis of metal concentration (unit: %).

	Size (μm)	Al	Ba	Ca	Cr	Cu	Fe	K	Mg	Mn	Pb	Sr	Ti	Zn	Mean	SD[b]
Slag A AC	<75	–	–	20.2	20.3	16.3	–	–	22.8	13.4	11.1	16.2	38.3	16.2	19.4	7.95
	75–150	–	–	41.0	37.8	29.8	–	–	37.6	32.4	26.5	36.7	31.7	32.6	34.0	4.58
	150–300	–	–	49.5	47.4	47.6	–	–	39.5	26.6	35.0	49.6	48.2	39.3	42.5	8.00
	300–600	–	–	55.2	53.0	55.9	–	–	56.5	37.0	38.3	57.7	58.8	41.6	50.4	8.85
	600–1000	–	–	50.2	52.9	47.9	–	–	60.8	43.1	35.4	51.6	47.5	23.4	45.9	10.9
	>1000	–	–	20.3	20.0	17.1	–	–	15.8	12.5	18.0	26.2	9.47	0[a]	15.5	7.52
Slag B AC	<75	19.3	19.2	25.9	20.7	6.08	–	13.8	27.6	–	–	21.7	18.0	–	19.1	6.39
	75–150	30.2	33.1	41.1	29.9	19.1	–	27.9	40.8	–	–	36.9	28.4	–	31.9	6.98
	150–300	36.4	39.8	48.1	45.1	48.0	–	36.0	40.2	–	–	42.6	43.2	–	42.2	4.47
	300–600	49.1	48.3	59.8	53.3	53.5	–	45.5	62.4	–	–	52.3	62.9	–	54.1	6.27
	600–1000	41.8	44.3	55.2	68.3	45.9	–	47.2	65.6	–	–	48.7	56.3	–	52.6	9.43
	>1000	3.39	14.2	18.7	15.5	15.2	–	20.1	17.9	–	–	16.7	6.96	–	14.3	5.57
Slag C AC	<75	–	–	27.9	23.1	6.98	9.06	–	–	6.03	9.02	–	–	17.1	14.2	8.64
	75–150	–	–	55.3	40.4	33.3	0[a]	–	–	8.05	27.1	–	–	42.8	29.6	19.6
	150–300	–	–	64.6	52.0	52.1	41.5	–	–	28.1	38.2	–	–	59.9	48.1	12.8
	300–600	–	–	67.9	56.5	97.6	64.1	–	–	44.4	59.6	–	–	58.7	64.1	16.5
	600–1000	–	–	63.0	47.6	30.1	52.9	–	–	46.1	31.9	–	–	36.4	44.0	11.9
	>1000	–	–	26.0	19.5	4.7	13.2	–	–	10.4	10.4	–	–	0[a]	12.0	8.73

[a] It assumed to be zero because calculation results were negative values.
[b] Standard deviation.

4. Conclusion

Abrasion test series were conducted for asphalt concretes containing only natural aggregates and 30 wt% of substituted slag aggregates. Two of three slag-asphalt concretes generated larger size and 1.5–3.0 times higher generation rate of abrasion dust than the reference asphalt concrete did. This suggests that the slag aggregates fragmentation depends on not only abrasion resistance of slag aggregate but also other factors like interlocking between slag aggregate and asphalt binder. The enrichment of slag-derived fragments in abrasion dust, estimated on the basis of the peak intensity of quartz and heavy metal concentrations, had size dependency for all slag-asphalt concretes. Slag-derived fragments were enriched in abrasion dust particles with diameters of 150–1000 μm and their enrichment factors were estimated to be 1.4–2.1. In contrast, there was no enrichment in abrasion dust particles with diameter less than 75 μm. This suggests that prior airborne-size fragmentation of substituted slag aggregates does not need to be considered for tested slag aggregates when environmental risks of abrasion dust of slag-asphalt pavement are assessed.

Acknowledgment

The authors appreciate the financial support by the Japan Society for the Promotion of Sciences (JSPS), the International Training Program "Formation of an Asian Center for Earth Resources and Environment Research for International Research Associates and Graduate Students" and Grant-in-Aid for Young Scientists (A) (23681014).

References

[1] Y. Xue, S. Wu, H. Hou, J. Zha, Experimental investigation of basic oxygen furnace slag used as aggregate in asphalt mixture, J. Hazard. Mater. 138 (2006) 261–268.
[2] D.H. Shen, C.M. Wu, J.C. Du, Laboratory investigation of basic oxygen furnace slag for substitution of aggregate in porous asphalt mixture, Construct. Build. Mater. 23 (2009) 453–461.
[3] P. Ahmedzade, B. Sengoz, Evaluation of steel slag coarse aggregate in hot mix asphalt concrete, J. Hazard. Mater. 165 (2009) 300–305.
[4] S. Li S, K. Zhu, S. Noureldin, Evaluation of friction performance of coarse aggregates and hot-mix asphalt pavements, J. Test. Eval. 35 (2007) 571–577.
[5] M. Kouda, Experimental pavement using household waste slag, Waste Manage. 16 (5/6) (1996) 461–474.
[6] N. Fukuzaki, T. Yanaka, Y. Urushiyama, Effects of studded tires on roadside airborne dust pollution in Niigata, Japan, Atmos. Environ. 20 (1986) 377–386.
[7] H. Trevahattu, K.J. Kupiainen, M. Räisänen, T. Mäkelä, R. Hillamo, Generation of urban road dust from anti-skid and asphalt concrete aggregates, J. Hazard. Mater. 132 (2006) 39–46.
[8] M. Raisanen, K. Kupiainen, H. Tervahattu, The effect of mineralogy, texture and mechanical properties of anti-skid and asphalt aggregates on urban dust, stages II and III, Bull. Eng. Geol. Environ. 64 (3) (2005) 247–256.
[9] F. Kehagia, Skid resistance performance of asphalt wearing courses with electric arc furnace slag aggregates, Waste Manage. Res. 27 (3) (2009) 288–294.
[10] K.H. Karstensen, W. Lund, Multielement analysis of city waste incineration ash and slag by inductively coupled plasma atomic emission spectrometry, Sci. Total Environ. 79 (2) (1989) 179–189.
[11] S. Abe, F. Kambayashi, M. Okada, Ash melting treatment by rotating type surface melting furnace, Waste Manage. 16 (5/6) (1996) 431–443.
[12] M. Nishigaki, Producing permeable blocks and pavement bricks from molten slag, Waste Manage. 20 (2/3) (2000) 185–192.
[13] A. Saffarzadeh, T. Shimaoka, Y. Motomura, K. Watanabe, Chemical and mineralogical evaluation of slag products derived from the pyrolysis/melting treatment of MSW, Waste Manage. 26 (12) (2006) 1443–1452.
[14] C.H. Jung, T. Matsuto, N. Tanaka, Behavior of metals in ash melting and gasification-melting of municipal solid waste (MSW), Waste Manage. 25 (3) (2005) 301–310.
[15] Y. Xiao, M. Oorsprong, Y. Yang, J.H.L. Voncken, Vitrification of bottom ash from a municipal solid waste incinerator, Waste Manage. 28 (6) (2008) 1020–1026.
[16] K.L. Lin, C.T. Chang, Leaching characteristics of slag from the melting treatment of municipal solid waste incinerator ash, J. Hazard. Mater. 135 (2006) 296–302.